

1 **MiRNAs profiling and degradome sequencing between the CMS-line N816S and**  
2 **its maintainer line Ning5m during anther development in pepper (*Capsicum***  
3 ***annuum* L.)**

4

5 Hongyuan Zhang, Shuping Huang, Jie Tan, Xia Chen, Min Zhang\*

6

7 Wuhan Academy of Agricultural Sciences, Wuhan, 430070, Hubei province, China.

8 \*Corresponding author: Min Zhang, email address: zhangmin818@aliyun.com

9

10 **Abstract**

11 Utilization of cytoplasmic male sterility (CMS) is significant for agriculture.  
12 MiRNAs are a class of endogenously non-coding small RNAs (21-24 nt) that play key  
13 roles in the regulation of various growth and developmental processes in plants. The  
14 knowledge miRNA-guided CMS regulation is rather limited in pepper. To better  
15 understand the miRNAs involvement and regulatory mechanism of CMS, miRNA  
16 libraries from anther of CMS-line N816S and its maintainer line Ning5m were  
17 generated by miRNAome sequencing in pepper. A total of 76 differentially expressed  
18 miRNAs were detected, of which 18 miRNAs were further confirmed by quantitative  
19 real-time PCR (qRT-PCR). In addition, miRNA targets were identified by degradome  
20 sequencing. The result showed that 1292 targets that were potentially cleaved by 321  
21 miRNAs (250 conserved miRNAs and 71 novel miRNAs). Gene Ontology (GO) and  
22 KEGG pathway analysis indicated that 35 differentially expressed miRNAs might  
23 play roles in the regulation of CMS sterility, by cleaving 77 target transcripts, such as  
24 *MYBs*, *SPLs*, and *AFRs*, of which targeted by miR156, miR167, miRNA858 family.  
25 Nineteen miRNA-cleaved targets were selectively examined by qRT-PCR, and the  
26 results showed that there were mostly negative correlations between miRNAs and  
27 their targets on the expression level. These findings provide a valuable information to  
28 understand miRNAs mechanism during anther development and CMS occurrence in  
29 pepper.

30

31 **Keywords:** CMS; miRNAome; degradome sequencing; miRNA regulation; Pepper

32 **Introduction**

33 MicroRNAs (miRNAs) are a class of endogenous non-coding small RNAs  
34 (sRNAs) with 21-24 nucleotides (nt) in animals and plants(Zhou et al., 2020). In  
35 plants, mature miRNA sequences were generated from primary miRNA transcripts  
36 (pri-miRNA) by Dicer-like (DCL1)(Zhang et al., 2015). The mature miRNAs are

37 incorporated into the RNA-induced silencing complex (RISC) to guiding the cleavage  
38 of specific complementary mRNAs(Schuck et al., 2013). MiRNAs are widely  
39 considered as negative-regulated gene expression at the post-transcription or  
40 translation process via degrading target mRNAs or repressing mRNA  
41 translation(Stepien et al., 2017). Previous studies have manifested that miRNAs  
42 involved in various plant growth and developmental processes, such as hormone  
43 homeostasis, flower development, embryogenesis and stress responses(Jha and  
44 Shankar, 2011;Pei et al., 2013).

45 Recently, a large number of studies have revealed miRNAs as important  
46 regulators of gene expressions to be involved in the developmental transition from  
47 vegetative growth to reproductive growth(Lin et al., 2013). MiR156 and miR172, two  
48 prime participators in flowering regulation, have been shown to regulate the floral  
49 transition in plant(Zhu and Helliwell, 2011;Yu et al., 2012;Diaz-Manzano et al., 2018).  
50 MiR156 could target SQUAMOSA Promoter Binding Protein-like (SPL)  
51 Transcription Factors (TF) and decreases with increasing life spans of the plant(Zheng  
52 et al., 2019). Overexpression of miR156 could delay flowering and prolong vegetative  
53 stage in many species, including Arabidopsis, rice and tomato(Zheng et al., 2019).  
54 The miR172, which targets APETALA2-like (*AP2*) transcription factors, has the  
55 opposite effect to the miR156 on the regulation of flowering time and increases with  
56 phase development and induces floral organogenesis and promote flowering(Tripathi  
57 et al., 2018). In addition, miR397 has been reported promoting panicle branching,  
58 increasing grain size, and resulting in improving yield in rice(Zhang et al., 2013).  
59 These studies showed that miRNAs play important roles in a number of  
60 developmental processes and pathways which regulate flower development related  
61 process.

62 Pepper (*Capsicum annuum* L.) is one of the most economically important  
63 worldwide vegetable crops(Barrajon-Catalan et al., 2020). Hybrid breeding has made  
64 a tremendous contribution to pepper yield, increasing seed production efficiency and  
65 protection of the varieties patent(Jifon et al., 2019). The utilization of male sterility in  
66 hybrid pepper is mainly based on three-line systems, which including cytoplasmic  
67 male sterile line (CMS), a maintainer line and restorer line(Bohra et al., 2016). In the  
68 CMS pepper, an ORF named *orf456*, was found at the 3'-end of the *coxII* gene, which  
69 is concluded that the *orf456* may represent a candidate gene, from mitochondrial  
70 genes, for determining the male-sterile phenotype of CMS(Kim et al., 2007).  
71 Furthermore, several CMS-related sterile genes and fertility restorer genes also have  
72 been cloned from various plants(Bohra et al., 2016). In Arabidopsis, miR167  
73 overexpression has been reported leading to male fertility defects(Ru et al., 2006),  
74 whereas miR159a overexpression results in decreased expression of *MYB33* and  
75 *MYB65*, leading to male sterility and delays flowering time(Anthony, 2005). With the  
76 development of miRNAome sequencing technology, differential expression patterns  
77 of miRNAs between the cytoplasmic male sterility (CMS) line and its maintainer line  
78 have been reported in many vegetable crops, such as Brassica juncea(Yang et al.,  
79 2013), Chinese cabbage(Wei et al., 2015) and Radish(Zhang et al., 2016b). A large  
80 number of miRNAs related to flowering and flower development have been identified

81 and characterized in above species. Nevertheless, there are no reports on systematic  
82 identification and characterization of CMS-related miRNAs in pepper.

83 To explore the roles of miRNA in CMS, we identified the miRNAs via a  
84 high-throughput sequencing approach from pepper anthers at the early uninucleate  
85 stage of the sterile line N816S and its maintainer line Ning5m. Differential expression  
86 patterns of miRNAs were analyzed and compared between N816S and Ning5m.  
87 Targets were predicted by degradome sequencing. These results may provide insights  
88 into clarification of the molecular mechanisms underlying the regulation of miRNAs  
89 during pollen development.

90

## 91 **Materials and Methods**

### 92 **Pepper materials**

93 The CMS sterile line N816S and its maintainer line Ning5m were used in this  
94 study. The plants were grown in greenhouse of the vegetable institute of Wuhan  
95 academy of agricultural sciences under normal conditions. In general, anthers at the  
96 uni-nucleate stage were manually collected. Anthers were harvested from three  
97 individual plants of each cultivar, immediately frozen in liquid nitrogen, stored at  
98 -80°C, and then used for RNA isolation. The microspore development was judged by  
99 both the floret length as described by Parra- Vega et al (Parra-Vega et al., 2013).

100

### 101 **Small RNA library Construction, sequencing, and miRNA analysis**

102 Total RNA was extracted using Trizol reagent (Invitrogen, CA, USA). RNA  
103 quantity was detected by Qubit Fluorometer (Invitrogen, CA, USA), and RNA purity  
104 was assayed by NanoDrop spectrophotometer (BioRad, PA, USA) and Agilent2100  
105 bioanalyzer (Agilent Technologies, CA, USA). According to the manufacturer's  
106 instructions, sRNA libraries were constructed using the Small RNA Sample Prep Kit  
107 (Illumina, CA, US) and meanwhile the sRNA passed quality test(Yeri et al., 2018).  
108 Briefly, the small RNA (18-30 nt) were ligated to a 3' adaptor and a 5' adaptor  
109 sequentially and then converted to cDNA by RT-PCR. The purified cDNAs after  
110 reverse transcription reaction were sequenced by the Illumina Hiseq2000 (Illumina,  
111 CA, USA). After the Illumina sequencing, the raw sequences were obtained through a  
112 quality control process to generate high quality reads, and clean reads were directly  
113 used for further bioinformatics analysis with ACGT101-v4.2-miR (LC Sciences, TX,  
114 USA) to remove adaptor sequences, junk reads, short reads, common RNA families  
115 (rRNA, tRNA, snRNA and snoRNA), repeats(Jeyaraj et al., 2019). Because of lacking  
116 known miRNA records of pepper in miRNA database (miRBase 21 released), unique  
117 sRNA sequences (18-25 nt) were mapped to specific species precursors in the  
118 miRBase 21 and the pepper reference sequence to identify conserved miRNAs by  
119 BLAST search. New miRNAs were identified by extracting flanking genome  
120 sequence of unique sRNAs using MIREAP (<http://sourceforge.net/projects/mireap/>)

121 (Huang et al., 2010), followed by the prediction of secondary structures by Mfold  
122 program (<http://unafold.rna.albany.edu/?q=mfold>) (Reuter and Mathews, 2009).

### 123 **Degradome Library Construction, Data analysis and Target identification**

124 The degradome library, a mixed samples' library, was constructed according to  
125 the method described previously using sliced ends of polyadenylated  
126 transcripts (German et al., 2009). In brief, poly-A-containing mRNA was purified from  
127 total RNA mixture of N816S and Ning5m, then ligated to 5' RNA adaptor containing  
128 a *MmeI* recognition site. Subsequently, RT-PCR was performed to first-strand cDNA,  
129 followed by digestion with *MmeI*, and then ligated to 3' adaptor. Finally, ligation  
130 product was amplified, purified and subjected to Illumina sequencing.

131 Raw reads were performed to remove adaptor sequence and low-quality reads  
132 resulting in clean reads. The high-quality specific sequences of were collected for  
133 subsequent degradome tags analysis. To identified potentially sliced targets of  
134 miRNAs, degradome sequence analysis were processed using the Cleveland 3.0  
135 software package and the ACGT301-DGE program (LC Sciences, TX, USA) (Gong et  
136 al., 2015). The tags, which mapped to sense cDNA, were used to predict cleavage  
137 sites. Height of the degradome peak at each occupied transcript position was placed  
138 into five possible categories.

### 139 **Quantitative real-time PCR (qRT-PCR) validation**

140 Total RNA was extracted from pepper anthers, and RNA-free DNase I  
141 (Fermentas, USA) was used to remove DNA contamination for 15 min at 37°C.  
142 Stem-loop qRT-PCR were carried out to validate differential expressional levels of  
143 miRNAs. The mRNA template for the miRNA target was reverse transcribed using  
144 the OligodT<sub>20</sub> primer for qRT-PCR. All miRNA detection primers were designed and  
145 synthesized based on the mature miRNA sequences. For each miRNA, approximately  
146 1 µg of total RNA was reverse-transcribed by reverse transcriptase using  
147 miRNA-specific stem-loop primers and a Fermentas Revert Aid First Strand cDNA  
148 Synthesis Kit (Fermentas, USA). Relative expression analysis of the miRNA and its  
149 target were performed using the ABI Step One Plus™ Real Time PCR System  
150 (Applied Biosystems, USA) and SYBR Green Master Mix (Roche, Germany). All  
151 reactions were run with three individual biological replicates, and *18S rRNA* was used  
152 as the internal control gene refer to Hwang et al (Hwang et al., 2013). The relative  
153 expression of miRNA and mRNA were used quantified the  $2^{-\Delta\Delta Ct}$  method to calculate  
154 the fold change between N816S and Ning5m (Asha et al., 2016). The primers used are  
155 listed in Table S1.

156

## 157 **Results**

### 158 **Overview of Small RNAs Libraries Sequencing Date**

159 To determine the involvement regulatory roles of miRNAs in the fertility of sterile  
160 and maintainer lines during anther development in pepper. Six small RNA libraries,  
161 including three biological replicates from N816S (N816S\_1, N816S\_2, N816S\_3) and  
162 Ning5m (Ning5m\_1, Ning5m\_2, Ning5m\_3), were constructed for deep sequencing.  
163 An average of 14,567,767 and 14,274,100 raw reads were obtained from N816S and  
164 Ning5m anthers, respectively, which after length, Junk reads, Rfam, Repeat, mRNA,  
165 rRNA, tRNA, snoRNA and snRNA reads filtering, an average of 10,780,898 (72.21%)  
166 valid reads representing 6,882,786 (84.68%) unique sequences and 10,442,445  
167 (74.25%) valid reads representing 6,666,094 (86.4%) unique reads, respectively  
168 (Table 1). The proportion of the valid reads in the corresponding raw reads was more  
169 than 70%, which suggested that the quality of the sequencing data was high (Table1).  
170 The length of total sRNAs and ranged from 18 to 25 nt, and in both the N816S and  
171 Ning5m libraries, the 24 nt category was most abundant (average of 55.83% and  
172 59.92% in N816S and Ning5m libraries, respectively) (Figure 1A-B). The length of  
173 unique sRNAs, in both the N816S and Ning5m libraries, the 24 nt category was most  
174 abundant (average of 59.15% and 62.90% in N816S and Ning5m libraries,  
175 respectively) (Figure 2C-D). This is consistent with the typical lengths of plant  
176 sRNAs reported in other studies(Asha et al., 2016;Hu et al., 2016).

### 177 **Conserved miRNAs and novel miRNAs identified in Pepper**

178 These unique sequences were subsequently used to identify conserved and novel  
179 miRNAs by alignment against miRBase (Version 22), the pepper genome and  
180 expressed sequence tag (EST) or pre-miRNA sequences. Unique miRNA transcripts  
181 identified from the mappable sequences are divided into five group types (Table  
182 S2)(Gong et al., 2015): (1) gp1a type: Unique reads map to specific  
183 miRNAs/pre-miRNAs in miRbase and the pre-miRNAs further map to the genome  
184 and EST. Total 77 miRNAs from the six samples corresponding to 50 known pepper  
185 pre-miRNAs (Table S2-1). (2) gp1a type: Reads map to selected (except for specific)  
186 miRNAs/pre-miRNAs in miRbase and the pre-miRNAs further map to the genome  
187 and EST. 122 miRNAs, which correspond to 94 known pepper pre-miRNAs, which  
188 cannot be mapped to genome or EST (Table S2-2). (3) gp2b type: Unique reads map  
189 to selected miRNAs/pre-miRNAs in miRbase. The mapped pre-miRNAs do not map  
190 to the genome, but the reads (and of course the miRNAs of the pre-miRNAs) map to  
191 genome. The extended genome sequences from the genome loci may form hairpins.  
192 261 miRNAs corresponding to 314 others known miRbase plant pre-miRNAs, which  
193 are mapped to genome or EST (Table S2-3). (4) gp3a type: Unique reads map to  
194 selected miRNAs/pre-miRNAs in miRbase. The mapped pre-miRNAs do not map to  
195 the genome, and the reads do not map to the genome; Forty miRNAs corresponding to  
196 35 others known miRbase plant pre-miRNAs, which cannot be mapped to genome or  
197 EST (Table S2-4). (5) gp4a: Unique reads do not map to selected pre-miRNAs in



198 miRBase, but the reads map to genome and the extended genome sequences from  
199 genome may form hairpins; 411 miRNAs corresponding to 421 candidate  
200 pre-miRNAs, which are predict RNA hairpins derived from genome or EST, and these  
201 miRNAs are novel miRNA, which are labeled PC (pepper candidate) (Table S2-5).

202 In the present study, identified mature miRNAs are divided into two type, including  
203 conserved miRNA and novel miRNA (Table 1), referring to the research of Maize(Li  
204 et al., 2017). The length of the mature miRNAs ranged from 18 to 25 nt. The 24 nt  
205 and 21 nt miRNA category was most abundant, 41.85% and 27.41%, respectively  
206 (Figure 2A). This is consistent with the typical lengths of plant sRNAs reported in  
207 other studies(Gao et al., 2016;Zhang et al., 2016a). Of the conserved miRNA 21-nt  
208 miRNAs were most abundant (37.32%) (Figure 2B), representing the dominant size  
209 of mature miRNAs in plants. The 5' terminal nucleotides of sRNA sequences  
210 influence classification of their AGO complexes and is an important feature affecting  
211 function(Schuck et al., 2013). Most miRNAs are incorporated into the AGO1 effector  
212 complex, resulting in sequence specificity that either cleaves or translationally  
213 represses their targets(Dalmadi et al., 2019). Therefore, we examined the 5' nucleotide  
214 distribution of conserved miRNAs, and 42.49% started with uridine at 5' -end, and  
215 26.17% started with adenine (Figure 2C).

216

## 217 **Differentially expressed miRNAs analysis between pepper sterile line N816S and** 218 **its maintainer line Ning5m**

219 MiRNAs are play an important role in plant development and apoptosis(Jovanovic  
220 and Hengartner, 2006;Wang et al., 2007). To determine differential expression  
221 between N816S and Ning5m anthers. MiRNA expression was normalized to  
222 transcripts per million and simplified as normalized expression (Norm)(Gong et al.,  
223 2015). A miRNA was considered if the Norm value was greater than one in the all  
224 given replicated samples. Based on this criterion, 525 miRNAs were detected (Figure  
225 3A), including a total of 350 conserved miRNAs (38.42% of the total miRNAs)  
226 belonging to 55 families were observed in at least one of the group samples (Table  
227 S3). In correlation analysis, Norm values of the N816S and Ning5m anthers were  
228 found to be highly correlated between repeats ( $r>0.99$ ), indicating good  
229 reproducibility of the miRNAome results (Figure S1).

230 A one-tailed t-test was used to identify differentially expressed miRNAs with p  
231 value  $< 0.05$ (Xing et al., 2012). The hierarchical clustering of the differential  
232 expression mRNAs was made and showed different expression patterns between the  
233 N816S and Ning5m (Figure 5A). As a result, a total of 76 miRNAs (59 conserved  
234 miRNAs and 17 novel miRNAs) were found to be differentially expressed between  
235 the two phenotypes (Table 3). Compared with the Ning5m, 44 miRNAs (34 conserved  
236 miRNAs and 10 novel miRNAs) were found to be down-regulated and 32 miRNAs  
237 (25 conserved miRNAs and 7 novel miRNAs) up-regulated in the N816S (Figure 3B).  
238 Nta-miR156g\_L+1 and stu-miR156a-5p had high expression abundance in  
239 MiRNA156 family, were down-regulated in sterile line N816S. However, miRNA390  
240 family, including hex-MIR390a-p5\_1ss21GT, hex-MIR390b-p5\_2ss10TC21GA and

241 hex-MIR390b-p5\_1ss21GT, were up-regulated in sterile line N816S. Five miRNAs  
242 (stu-miR393-3p, stu-miR399j-3p\_1ss21GA, nta-miR6149a\_L+1R-1\_1ss21GC and  
243 stu-miR398b-3p ath-miR8175\_L+4) were specifically expressed in Ning5m. Five  
244 miRNA(nta-MIR172e-p3\_2ss15CG19TA,ppe-MIR399a-p3\_2ss5AT18TC,ppe-MIR39  
245 9a-p5\_2ss5AT18TC, stu-miR3627-5p\_R-1 and sly-MIR10528-p3\_2ss9GA19TC)  
246 were specifically expressed in N816S. To validate conserved miRNAs identified and  
247 novel miRNAs predicted, we selected 18 differential expressed miRNAs for  
248 stem-loop qRT-PCR. The expression trends of these miRNAs were consistent with the  
249 high-throughput sequencing results. As showed in Figure 3C, expression of these  
250 miRNAs from qRT-PCR displayed a similar tendency with those from small RNA  
251 sequencing.

252

### 253 **Targets analysis of miRNAs in anthers of Pepper.**

254 To understand the function of the mature miRNAs from anthers of Pepper,  
255 targets of miRNAs were detected using degradome sequencing technology. A total of  
256 34233673 (99.24%) mappable reads from raw reads were obtained, including  
257 12320360(99.19%) unique mappable reads, while 20851831 (60.45%) transcript  
258 mapped reads, including 6635426(53.42%) unique transcript mappable reads, were  
259 obtained (Table S4). The target transcripts were sorted into five categories according  
260 to the relative abundance of the tags at the target mRNA sites(Gong et al., 2015):  
261 category “0” is defined as >1 raw read at the position, with abundance at a position  
262 equal to the maximum on the transcript and with only one maximum on the transcript;  
263 category “1”, the expected cleavage signature was equal to the maximum on the  
264 transcript and more than one maximum position on the transcript; category “2”,  
265 abundance at the position was less than the maximum but higher than the median for  
266 the transcript; category “3”, the abundance at the position equal to or less than the  
267 median for the transcript; category “4”, abundance at the position was only one raw  
268 read. Figure 6 showed the typical five categories of the target transcripts.

269 A total of 1292 reliable targets ( $p$ -value <1) that were potentially cleaved by  
270 321 miRNAs (250 conserved miRNAs and 71 novel miRNAs) were identified (Table  
271 S5). A total of 77 target genes were identified to be targeted by 35 differentially  
272 expressed miRNAs (27 conserved miRNAs and 8 novel miRNAs) (Table S6). Many  
273 targets of miR156, miR167, miRNA858 families were identified as transcription  
274 factors, such as SPL, ARF, and MYB, respectively, which have been experimentally  
275 validated by the previous studies.

### 276 **Gene Ontology (GO) and KEGG Pathway Analysis of Targets.**

277 The targets were annotated using the GO annotations analysis, which is  
278 commonly used to describe the function of genes and gene products, meanwhile the  
279 KEGG analysis is used to provide the pathway of annotated targets. Figure 5B

280 showed the GO functional classification of miRNA targets in the pepper anthers.  
281 Targets covered a broad range of functional categories. However, targets of DNA  
282 binding, regulation of transcription-, and DNA-templated genes, transcription factor  
283 activity-, and sequence-specific DNA binding, transcription-, and DNA-templated  
284 genes were mostly enriched. This suggested that those target genes may play an  
285 important role in pepper anthers. The pathways of all the miRNAs and targets  
286 involved were listed (Table S7). There were 107 pathways that targets involved, while  
287 carbohydrate metabolism, translation, folding sorting and degradation pathways  
288 owned most targets (Figure 5C). Furthermore, the 77 miRNA targets from 35  
289 differentially expressed miRNAs were found to be involved in multiple pathways,  
290 including plant hormone signal transduction, purine metabolism, starch and sucrose  
291 metabolism, oxidative phosphorylation, and others (Table S8).  
292

### 293 **Expression profiles of miRNA targets examined by qRT-PCR**

294 To examine the correlation between the targets and the corresponding miRNAs,  
295 the expression levels of 19 selected targets were examined by qRT-PCR analysis.  
296 MiRNAome sequencing result showed that miRNA156a/g (stu-miR156a and  
297 nta-miR156g\_L+1), miRNA167a/h (stu-miR167a-5p, stu-miR167a-5p\_1ss21AT and  
298 mdm-miR167h\_1ss22AT), stu-miR393-5p and nta-miR6149a\_L+1R-1\_1ss21GC  
299 were down-regulated in N816S compare to Ning5m (Table 3). The degradome  
300 sequencing results indicate that miRNA156a/g target SPL family genes (SPL3, SPL6  
301 and SPL9), miRNA167a/h (aly-miR167a-5p\_R+1\_1ss21AT, gma-miR167a\_1ss21AT,  
302 mdm-miR167h\_1ss22AT, stu-miR167a-5p\_1ss21AT) targets an AUXIN RESPONSE  
303 FACTOR gene (ARF8), MiRNA393 targets two AUXIN SIGNALING F-box  
304 genes (TIR1 and AFB2) (Table S8). QRT-PCR analysis showed that the expression  
305 profiles of the above miRNA targets were up-regulated in N816S (Figure 6A).

306 In contrast, miRNA159\_R3, nta-MIR169j-p3\_2ss8GA19CT,  
307 stu-miR319b\_L+1R-1, hex-MIR390a-p5\_1ss21GT, ppe-MIR399a-p3\_2ss5AT18TC,  
308 ppe-MIR858-p5\_1ss4GA, cst-MIR11334-p5\_2ss9TG18TC and PC-5p-154497\_29  
309 were up-regulated in N816S (Table 3). MiRNA159\_R3 targets a plasma membrane  
310 H<sup>+</sup>-ATPase gene (*ACA13*), a  $\gamma$ -TuC Protein 3 (GCP3)-Interacting Protein gene (*GIP1*),  
311 MiRNA169j-p3 targets a heat shock protein gene (HSP70), MiRNA319b targets four  
312 TEOSINTE BRANCHED/CYCLOIDEA/PCF transcription factor genes (*TCP2*,  
313 *TCP4*, *TCP24*) and a Aldehyde dehydrogenase gene (*ALDH6B2*), MiRNA390a-p5  
314 targets a GDP dissociation inhibitor gene (*GDI1*), miRNA399a-p3 targets a  
315 ceramide-1-phosphate transfer protein gene (*ACD11*), miRNA858-p5 targets several  
316 MYB protein genes (*MYB3*, *MYB4*, *MYB12* and *MYB80*), miR11334-p5 targets a  
317 phospholipase D alpha 1-like gene (*PLD1*) and a Acyl-CoA oxidase gene (*ACX1*), and  
318 a novel miRNA of PC-5p-154497\_29 targets a UDP-galactose-dependent  
319 digalactosyldiacylglycerol synthase gene (*DGD2*) (Table S8). Most of above targets  
320 were down-regulated in N816S (Figure 6B).

321 Most negative correlations were found between the expression levels of the



322 target genes and their corresponding miRNAs in anthers of the sterile line N816S and  
323 its maintainer line Ning5m, implying that miRNA-mediated mRNA silencing  
324 occurred during anther development.  
325

## 326 **Discussion**

327 Several studies have shown that miRNAs regulate anther development in  
328 plants (Yang et al., 2013; Gong et al., 2015). However, few studies on the relationships  
329 between miRNA biogenesis and CMS occurrence during anther development in  
330 pepper were very limited. MiRNAome and degradation sequencing technology  
331 provides an effective way to identify and evaluate the expression profiles of miRNAs  
332 and targets associated with CMS occurrence in plant tissues during anther  
333 development (Wei et al., 2015; Hu et al., 2016; Bai et al., 2017). To explore the roles of  
334 miRNAs during the occurrence of CMS, anthers at the early uninucleate stage were  
335 used to examine the expression profiles of the miRNAs in the sterile line N816S and  
336 its maintainer line Ning5m using high-throughput sequencing. To the best of our  
337 current knowledge, this study is the first report on identification and characterization  
338 of miRNAs, and their targets between a sterile line and its maintainer line during  
339 anther development in pepper.

340 In this study, a total of 76 miRNAs (59 conserved miRNAs and 17 novel  
341 miRNAs) were identified as differentially expressed between the sterile line N816S  
342 and its maintainer line Ning5m. To understand the function of the miRNAs from  
343 anthers of Pepper, targets of miRNAs were detected using degradome sequencing  
344 technology. From those targets, 80 target genes were identified to be targeted by 35  
345 differentially expressed miRNAs (27 conserved miRNAs and 8 novel miRNAs). The  
346 qRT-PCR results indicated that most negative correlations were found between the  
347 expression levels of the target genes and their corresponding miRNAs in the anthers  
348 of the sterile line N816S and its maintainer line Ning5m. KEGG analysis showed that  
349 most gene targets of the 35 differentially expressed miRNAs were involved in  
350 pathways, including plant hormone signal transduction, starch and sucrose  
351 metabolism, oxidative phosphorylation, purine metabolism, and others.

352 Intriguingly, a number of genes in hormone signaling were confirmed or  
353 predicted as targets of miRNAs. Auxin regulates anther dehiscence, pollen maturation,  
354 and filament elongation in *Arabidopsis*. The miR167-guided cleavage of auxin  
355 response factor *ARF8*, miR393-guided cleavage of auxin receptor *TIR1* and *AFB2*,  
356 and miR319-guided cleavage of jasmonate acid biosynthesis related transcription factor  
357 genes *TCPs*, which were reported in previous study (Liu and Chen, 2009). In  
358 *Arabidopsis*, loss of miR167 regulation in *mARF6* and *mARF8* expression caused  
359 arrested ovule development and anther indehiscence (Wu et al., 2006). Four auxin  
360 receptor-encoding genes, *TIR1*, *AFB1*, *AFB2*, and *AFB3*, are transcribed in anthers  
361 only during late stages of development starting at the end of meiosis (Shimizu-Mitao  
362 and Kakimoto, 2014). Up-regulation of *TIR1* enhances auxin sensitivity, and causes

363 altered leave phenotype and delayed flowering in *Arabidopsis*(Chen et al., 2011).  
364 MicroRNA319-regulated TCPs can activate CO transcription and control flowering  
365 time, shaping flower structure, leaf morphology, and plant architecture in  
366 *Arabidopsis*(Chen et al., 2011). In this study, up-regulation *AFR8* was targeted by  
367 down-regulated miRNA393a/h, up-regulated *TIR1* and *AFB2* were targeted by  
368 down-regulated miR393a, and down-regulated *TCPs* (*TCP2* and *TCP4*) were targeted  
369 by up-regulated miRNA393b, indicating might modulate the hormone response to  
370 play roles in the pollen development and CMS occurrence.

371 Targets of these differentially expressed miRNAs containing important  
372 transcription factors (TFs) and functional proteins are involved in many biological  
373 processes, including signal transduction, floral organ development, and organellar  
374 gene expression(Liu and Chen, 2009). For instance, miR156 targets *SPL* transcription  
375 factor family, which is regulatory functions throughout the growth and development  
376 stages in plants. Previous report showed that miR156 regulates the timing of flower  
377 formation vis *SPL3/4/5*, activating the expression of *LEAFY*, *FRUITFULL* and  
378 *APETALA*(Jung et al., 2011). In *Arabidopsis*, multiple *SPL* genes regulate cell  
379 division, differentiation and can result in fertile flower(Zheng et al., 2019). In this  
380 study, *SPL3*, *SPL6* and *SPL9* were identified as potentially targets of miR156 miRNA  
381 family members (stu-miR156a, stu-miR156a, nta-miR156g\_L+1) were identified as  
382 approximately triple up-regulated in N816S compared with Ning5M (Figure 6A),  
383 leading to disordered floral organ development in pepper, indicating that miR156 may  
384 participate in fertility regulation. Furthermore, miR858 targets *MYB* transcription  
385 factor family, which is involved in the control of plant development, determination of  
386 cell fate and identity, primary, and secondary metabolism. In rice, anther and pollen  
387 defect in floral organ development are found in the loss-of-function mutations of *MYB*.  
388 In *Arabidopsis*, *AtMYB3*, *AtMYB4*, *AtMYB7* and *AtMYB32* encode transcriptional  
389 repressors, and *AtMYB4* controls sinapate ester biosynthesis, whereas *AtMYB32*  
390 regulates pollen wall composition, and *AtMYB12* is involved in the regulation of  
391 flavonoid biosynthesis control flavonol biosynthesis(Dubos et al., 2010). The  
392 transcriptional activity of the PtMYB4 protein is positively regulated by the  
393 mitogen-activated protein kinase (MAPK) PtMAPK6 in *Pinus taeda*, which  
394 phosphorylates a Ser in the C terminal activation domain. In addition, *AtMYB80*  
395 regulated exine formation and acts downstream of *AtMYB35* to control anther  
396 development and/ or functionalities. In this present study, up-regulated miRNA858  
397 might via reducing transcript expression of *MYB3*, *MYB4*, *MYB12* and *MYB80*,  
398 leading to anther and pollen defect. In addition, MIR169j targets a heat shock protein  
399 *HSP70*, which has been widely involved in the protein peptides folding, assembly and  
400 transports, and the degradation of abnormal proteins. Studies have found that *HSP70*  
401 is associated with male sterility in plant and animal. Down regulation of *HSP70*  
402 expression level prolongs the duration of heat-induced male sterility in *Drosophila*  
403 *buzzatii*(Sarup et al., 2004). *HSP70* antisense RNA expression leads to male sterility  
404 in rice(Liu et al., 2008). In this study, up-regulated miRNA169j may through via  
405 reducing transcript expression of *HSP70*, leading to pollen abortion.

406 Many miRNA-targeted genes were involved in lipid transport and metabolism,

407 such as *PLD1/ACX1*, *ACA13/GIP*, *ALDH6*, *GDI1* and *DGD2*, which are cleaved by  
408 miR11334, miR159\_R-3, miR319b, miRNA390b and PC-5p-154497\_29, respectively.  
409 Those miRNAs may throughout their targets be involved in CMS sterile process.  
410 Phospholipase D alpha 1-like (PLD1) has been identified as cytosolic protein, which  
411 regulated cytosolic lipid droplet formation(Andersson et al., 2006). Acyl-CoA oxidase  
412 (ACX) was the first and the key step controlling enzyme involved in fatty acid  
413  $\beta$ -oxidation, and mutation of *ACX1* led to petal degeneration in Chinese  
414 Cabbage(Zheng et al., 2019). In plant, *ALDH6B2* encodes a methylmalonyl  
415 semialdehyde dehydrogenase, of which involved in the degradation of valine to  
416 propionyl CoA(Brockner et al., 2013). In addition, Plant cells have multiple plasma  
417 membrane (PM)-localized calcium ATPases (ACAs) pumping calcium ions out of the  
418 cytosol. The loss of ACA13 combination with a reduction in function of other ACAs  
419 leads to seedling death at bolting, revealing the essential role of their collective  
420 function in plant growth(Yu et al., 2018). Moreover, the  $\gamma$ -tubulin complex ( $\gamma$ -TuC)  
421 Protein 3 (GCP3)-Interacting Protein 1 (GIP1) is the smallest  $\gamma$ -TuC component  
422 identified. In Arabidopsis, *AtGIP1* and its homologous protein *AtGIP2* mutants are  
423 impaired in establishing a fully functional mitotic spindle and exhibit severe  
424 developmental defects(Batzenschlager et al., 2013). The GDP dissociation inhibitor  
425 protein GDI1 relates to control vesicle number and transport in an amelioration of  
426 zinc toxicity, allowing yeast to survive in the presence of toxic(Ezaki and Nakakihara,  
427 2012). Furthermore, Digalactosyl-diacylglycerol (DGD) is one of the major lipids  
428 found predominantly in the photosynthetic membrane of higher plants. *OsDGD2 $\beta$*  is  
429 the sole DGDG synthase gene highly expressed in anther, and its mutation confers  
430 male sterility with pale yellow and shrunken anther, devoid of starch granules in  
431 pollen, and delayed degeneration of tapetal cells in rice(Basnet et al., 2019). All above  
432 related miRNAs are up-regulated in sterile line N816S compare to its maintainer  
433 Ning5m and those disorder miRNA-targeted genes perhaps leading to  
434 membrane-disruptive effects and cell apoptosis.

435

## 436 **Conclusion**

437 In the present study, small RNA libraries from anther of CMS-line N816S and its  
438 maintainer line Ning5m were generated by small RNA sequencing in pepper. A total  
439 of 76 differentially expressed miRNAs were discovered, of which 18 were further  
440 confirmed by real-time quantitative PCR (qRT-PCR). Furthermore, targets of  
441 miRNAs were identified by degradome sequencing. A total of 1292 targets that were  
442 potentially cleaved by 321 miRNAs (250 conserved miRNAs and 71 novel miRNAs)  
443 were identified. Gene Ontology (GO) and KEGG pathway analysis of target  
444 transcripts indicated that 77 target genes cleaved by 35 differentially expressed  
445 miRNAs might play roles in the regulation of CMS sterility, such as MYB, SPL, and  
446 AFR family proteins targeted by miR156, miR167, miRNA858 family. Nineteen

447 targets were selectively examined by qRT-PCR, and the results showed that there was  
448 a negative correlation on the expression patterns between miRNAs and their targets.  
449 These findings provide valuable information to understand the roles of miRNAs  
450 during anther development and CMS occurrence in pepper.

#### 451 **Author contributions**

452 Min Zhang designed the study. Hongyuan Zhang, Shuping Huang and Jie Tan  
453 carried out the experiment, data analysis, interpretation of the results. Hongyuan  
454 Zhang drafted the manuscript. Xia Chen supervised the work and revised the  
455 manuscript. All authors have read and approved the final version of this submission.  
456

#### 457 **Acknowledgement**

458 This work was financially supported by the National Natural Science Foundation of  
459 China (Grant No. 31701936) and the subproject of National key research and  
460 development Program of China (2017YFD0101904).  
461

#### 462 **Reference**

- 463 Andersson, L., Bostrom, P., Ericson, J., Rutberg, M., Magnusson, B., Marchesan, D., Ruiz, M.,  
464 Asp, L., Huang, P., Frohman, M.A., Boren, J., and Olofsson, S.O. (2006). PLD1 and  
465 ERK2 regulate cytosolic lipid droplet formation. *J Cell Sci* 119, 2246-2257.
- 466 Anthony, A.M.F., G. (2005). The Arabidopsis GAMYB-Like Genes, MYB33 and MYB65 , Are  
467 MicroRNA-Regulated Genes That Redundantly Facilitate Anther Development. *The*  
468 *Plant Cell* 17, 705-721.
- 469 Asha, S., Sreekumar, S., and Soniya, E.V. (2016). Unravelling the complexity of  
470 microRNA-mediated gene regulation in black pepper (*Piper nigrum* L.) using  
471 high-throughput small RNA profiling. *Plant Cell Reports* 35, 53-63.

- 472 Bai, J.F., Wang, Y.K., Wang, P., Duan, W.J., Yuan, S.H., Sun, H., Yuan, G.L., Ma, J.X., Wang,  
473 N., Zhang, F.T., Zhang, L.P., and Zhao, C.P. (2017). Uncovering Male Fertility  
474 Transition Responsive miRNA in a Wheat Photo-Thermosensitive Genic Male Sterile  
475 Line by Deep Sequencing and Degradome Analysis. *Frontiers In Plant Science* 8.
- 476 Barrajon-Catalan, E., Alvarez-Martinez, F.J., Borrás, F., Perez, D., Herrero, N., Ruiz, J.J., and  
477 Micol, V. (2020). Metabolomic analysis of the effects of a commercial complex  
478 biostimulant on pepper crops. *Food Chemistry* 310.
- 479 Basnet, R., Hussain, N., and Shu, Q. (2019). OsDGD2 $\beta$  is the Sole Digalactosyldiacylglycerol  
480 Synthase Gene Highly Expressed in Anther, and its Mutation Confers Male Sterility in  
481 Rice. *Rice* 12, 66.
- 482 Batzenschlager, M., Masoud, K., Janski, N., Houlné, G., Herzog, E., Evrard, J.-L., Baumberger,  
483 N., Ehrardt, M., Nominé, Y., Kieffer, B., Schmit, A.-C., and Chabouté, M.-E. (2013).  
484 The GIP gamma-tubulin complex-associated proteins are involved in nuclear  
485 architecture in *Arabidopsis thaliana*. *Frontiers in Plant Science* 4.
- 486 Bohra, A., Jha, U.C., Adhimoolam, P., Bisht, D., and Singh, N.P. (2016). Cytoplasmic male  
487 sterility (CMS) in hybrid breeding in field crops. *Plant Cell Reports* 35, 967-993.
- 488 Brocker, C., Vasiliou, M., Carpenter, S., Carpenter, C., Zhang, Y., Wang, X., Kotchoni, S.O.,  
489 Wood, A.J., Kirch, H.-H., Kopečný, D., Nebert, D.W., and Vasiliou, V. (2013).  
490 Aldehyde dehydrogenase (ALDH) superfamily in plants: gene nomenclature and  
491 comparative genomics. *Planta* 237, 189-210.
- 492 Chen, Z.H., Bao, M.L., Sun, Y.Z., Yang, Y.J., Xu, X.H., Wang, J.H., Han, N., Bian, H.W., and  
493 Zhu, M.Y. (2011). Regulation of auxin response by miR393-targeted transport inhibitor



494 response protein 1 is involved in normal development in Arabidopsis. *Plant Molecular*  
495 *Biology* 77, 619-629.

496 Dalmadi, A., Gyula, P., Balint, J., Szittyá, G., and Havelda, Z. (2019). AGO-unbound cytosolic  
497 pool of mature miRNAs in plant cells reveals a novel regulatory step at AGO1 loading.  
498 *Nucleic Acids Research* 47, 9803-9817.

499 Diaz-Manzano, F.E., Cabrera, J., Ripoll, J.J., Del Olmo, I., Andres, M.F., Silva, A.C., Barcala,  
500 M., Sanchez, M., Ruiz-Ferrer, V., De Almeida-Engler, J., Yanofsky, M.F., Pineiro, M.,  
501 Jarillo, J.A., Fenoll, C., and Escobar, C. (2018). A role for the gene regulatory module  
502 microRNA172/TARGET OF EARLY ACTIVATION TAGGED 1/FLOWERING LOCUS  
503 T (miRNA172/TOE1/FT) in the feeding sites induced by *Meloidogyne javanica* in  
504 *Arabidopsis thaliana*. *New Phytologist* 217, 813-827.

505 Dubos, C., Stracke, R., Grotewold, E., Weisshaar, B., Martin, C., and Lepiniec, L. (2010). MYB  
506 transcription factors in Arabidopsis. *Trends in Plant Science* 15, 573-581.

507 Ezaki, B., and Nakakihara, E. (2012). Possible involvement of GDI1 protein, a GDP  
508 dissociation inhibitor related to vesicle transport, in an amelioration of zinc toxicity in  
509 *Saccharomyces cerevisiae*. *Yeast* 29, 17-24.

510 Gao, S., Yang, L., Zeng, H.Q., Zhou, Z.S., Yang, Z.M., Li, H., Sun, D., Xie, F.L., and Zhang,  
511 B.H. (2016). A cotton miRNA is involved in regulation of plant response to salt stress.  
512 *Scientific Reports* 6.

513 German, M.A., Luo, S.J., Schroth, G., Meyers, B.C., and Green, P.J. (2009). Construction of  
514 Parallel Analysis of RNA Ends (PARE) libraries for the study of cleaved miRNA targets  
515 and the RNA degradome. *Nature Protocols* 4, 356-362.

- 516 Gong, S.M., Ding, Y.F., Huang, S.X., and Zhu, C. (2015). Identification of miRNAs and Their  
517 Target Genes Associated with Sweet Corn Seed Vigor by Combined Small RNA and  
518 Degradome Sequencing. *Journal Of Agricultural And Food Chemistry* 63, 5485-5491.
- 519 Hu, J.H., Jin, J., Qian, Q., Huang, K.K., and Ding, Y. (2016). Small RNA and degradome  
520 profiling reveals miRNA regulation in the seed germination of ancient eudicot *Nelumbo*  
521 *nucifera*. *Bmc Genomics* 17.
- 522 Huang, Q.X., Cheng, X.Y., Mao, Z.C., Wang, Y.S., Zhao, L.L., Yan, X., Ferris, V.R., Xu, R.M.,  
523 and Xie, B.Y. (2010). MicroRNA Discovery and Analysis of Pinewood Nematode  
524 *Bursaphelenchus xylophilus* by Deep Sequencing. *Plos One* 5.
- 525 Hwang, D.G., Park, J.H., Lim, J.Y., Kim, D., Choi, Y., Kim, S., Reeves, G., Yeom, S.I., Lee,  
526 J.S., Park, M., Kim, S., Choi, I.Y., Choi, D., and Shin, C. (2013). The Hot Pepper  
527 (*Capsicum annuum*) MicroRNA Transcriptome Reveals Novel and Conserved Targets:  
528 A Foundation for Understanding MicroRNA Functional Roles in Hot Pepper. *Plos One*  
529 8.
- 530 Jeyaraj, A., Wang, X.W., Wang, S.S., Liu, S.R., Zhang, R., Wu, and Wei, C.T. (2019).  
531 Identification of Regulatory Networks of MicroRNAs and Their Targets in Response to  
532 *Colletotrichum gloeosporioides* in Tea Plant (*Camellia sinensis* L.). *Frontiers In Plant*  
533 *Science* 10.
- 534 Jha, A., and Shankar, R. (2011). Employing machine learning for reliable miRNA target  
535 identification in plants. *Bmc Genomics* 12.
- 536 Jifon, J., Crosby, K., Patil, B., and Leskovar, D. (2019). Effects of Potassium Nutrition on Seed  
537 Yield and Quality of Hybrid Chili Pepper (*Capsicum annuum* L.). *Hortscience* 54,

- 538 S395-S395.
- 539 Jovanovic, M., and Hengartner, M.O. (2006). miRNAs and apoptosis: RNAs to die for.  
540 *Oncogene* 25, 6176-6187.
- 541 Jung, J.-H., Seo, P.J., Kang, S.K., and Park, C.-M. (2011). miR172 signals are incorporated  
542 into the miR156 signaling pathway at the SPL3/4/5 genes in Arabidopsis  
543 developmental transitions. *Plant Molecular Biology* 76, 35-45.
- 544 Kim, D.H., Kang, J.G., and Kim, B.D. (2007). Isolation and characterization of the cytoplasmic  
545 male sterility-associated orf456 gene of chili pepper (*Capsicum annuum* L.). *Plant Mol*  
546 *Biol* 63, 519-532.
- 547 Li, H.P., Peng, T., Wang, Q., Wu, Y.F., Chang, J.F., Zhang, M.B., Tang, G.L., and Li, C.H.  
548 (2017). Development of Incompletely Fused Carpels in Maize Ovary Revealed by  
549 miRNA, Target Gene and Phytohormone Analysis. *Frontiers In Plant Science* 8.
- 550 Lin, C.S., Chen, J.J.W., Huang, Y.T., Hsu, C.T., Lu, H.C., Chou, M.L., Chen, L.C., Ou, C.I.,  
551 Liao, D.C., Yeh, Y.Y., Chang, S.B., Shen, S.C., Wu, F.H., Shih, M.C., and Chan, M.T.  
552 (2013). Catalog of *Erycina pusilla* miRNA and categorization of reproductive  
553 phase-related miRNAs and their target gene families. *Plant Molecular Biology* 82,  
554 193-204.
- 555 Liu, L., Liu, G.Q., and Hou, N. (2008). Construction and identification of HSP70 antisense RNA  
556 expression vector for genetic engineering male sterility in plant. *Anhui Agricultural*  
557 *Science and Technology* 9, 84, 128.
- 558 Liu, Q., and Chen, Y.Q. (2009). Insights into the mechanism of plant development: Interactions  
559 of miRNAs pathway with phytohormone response. *Biochemical And Biophysical*

- 560            *Research Communications* 384, 1-5.
- 561    Parra-Vega, V., Gonzalez-Garcia, B., and Segui-Simarro, J.M. (2013). Morphological markers  
562            to correlate bud and anther development with microsporogenesis and  
563            microgametogenesis in pepper (*Capsicum annuum* L.). *Acta Physiologiae Plantarum*  
564            35, 627-633.
- 565    Pei, H.X., Ma, N., Chen, J.W., Zheng, Y., Tian, J., Li, J., Zhang, S., Fei, Z.J., and Gao, J.P.  
566            (2013). Integrative Analysis of miRNA and mRNA Profiles in Response to Ethylene in  
567            Rose Petals during Flower Opening. *Plos One* 8.
- 568    Reuter, J., and Mathews, D.H. (2009). RNAstructure: Software for RNA Secondary Structure  
569            Prediction and Analysis. *Journal Of Biomolecular Structure & Dynamics* 26, 831-832.
- 570    Ru, P., Xu, L., Ma, H., and Huang, H. (2006). Plant fertility defects induced by the enhanced  
571            expression of microRNA167. *Cell Research* 16, 457-465.
- 572    Sarup, P., Dahlggaard, J., Norup, A.M., Jorgensen, K.T., Hebsgaard, M.B., and Loschcke, V.  
573            (2004). Down regulation of Hsp70 expression level prolongs the duration of  
574            heat-induced male sterility in *Drosophila buzzatii*. *Functional Ecology* 18, 365-370.
- 575    Schuck, J., Gursinsky, T., Pantaleo, V., Burgyan, J., and Behrens, S.E. (2013).  
576            AGO/RISC-mediated antiviral RNA silencing in a plant in vitro system. *Nucleic Acids*  
577            *Research* 41, 5090-5103.
- 578    Shimizu-Mitao, Y., and Kakimoto, T. (2014). Auxin Sensitivities of All Arabidopsis Aux/IAAs for  
579            Degradation in the Presence of Every TIR1/AFB. *Plant And Cell Physiology* 55,  
580            1450-1459.
- 581    Stepien, A., Knop, K., Dolata, J., Taube, M., Bajczyk, M., Barciszewska-Pacak, M., Pacak, A.,

- 582 Jamolowski, A., and Szweykowska-Kulinska, Z. (2017). Posttranscriptional  
583 coordination of splicing and miRNA biogenesis in plants. *Wiley Interdisciplinary*  
584 *Reviews-Rna* 8.
- 585 Tripathi, R.K., Bregitzer, P., and Singh, J. (2018). Genome-wide analysis of the SPL/miR156  
586 module and its interaction with the AP2/miR172 unit in barley. *Scientific Reports* 8.
- 587 Wang, Y., Stricker, H.M., Gou, D., and Liu, L. (2007). MicroRNA: past and present. *Front*  
588 *Biosci* 12, 2316-2329.
- 589 Wei, X.C., Zhang, X.H., Yao, Q.J., Yuan, Y.X., Li, X.X., Wei, F., Zhao, Y.Y., Zhang, Q., Wang,  
590 Z.Y., Jiang, W.S., and Zhang, X.W. (2015). The miRNAs and their regulatory networks  
591 responsible for pollen abortion in Ogura-CMS Chinese cabbage revealed by  
592 high-throughput sequencing of miRNAs, degradomes, and transcriptomes. *Frontiers*  
593 *In Plant Science* 6.
- 594 Wu, M.F., Tian, Q., and Reed, J.W. (2006). Arabidopsis microRNA167 controls patterns of  
595 ARF6 and ARF8 expression, and regulates both female and male reproduction.  
596 *Development* 133, 4211-4218.
- 597 Xing, R.H., Lussier, Y.A., Salama, J.K., Khodarev, N.N., Huang, Y., Zhang, Q.B., Khan, S.A.,  
598 Yang, X.N., Hasselle, M.D., Darga, T.E., Malik, R., Fan, H.L., Perakis, S., Filippo, M.,  
599 Corbin, K., Lee, Y., Posner, M.C., Chmura, S.J., Hellman, S., and Weichselbaum, R.R.  
600 (2012). MicroRNA expression characterizes oligometastasis(es). *Cancer Research*  
601 72.
- 602 Yang, J., Liu, X., Xu, B., Zhao, N., Yang, X., and Zhang, M. (2013). Identification of miRNAs  
603 and their targets using high-throughput sequencing and degradome analysis in



604 cytoplasmic male-sterile and its maintainer fertile lines of Brassica juncea. *BMC*  
605 *Genomics* 14, 9.

606 Yeri, A., Courtright, A., Danielson, K., Hutchins, E., Alsop, E., Carlson, E., Hsieh, M., Ziegler,  
607 O., Das, A., Shah, R.V., Rozowsky, J., Das, S., and Van Keuren-Jensen, K. (2018).  
608 Evaluation of commercially available small RNASeq library preparation kits using low  
609 input RNA. *Bmc Genomics* 19.

610 Yu, H., Yan, J., Du, X., and Hua, J. (2018). Overlapping and differential roles of plasma  
611 membrane calcium ATPases in Arabidopsis growth and environmental responses. *J*  
612 *Exp Bot* 69, 2693-2703.

613 Yu, S., Galvao, V.C., Zhang, Y.C., Horrer, D., Zhang, T.Q., Hao, Y.H., Feng, Y.Q., Wang, S.,  
614 Schmid, M., and Wang, J.W. (2012). Gibberellin Regulates the Arabidopsis Floral  
615 Transition through miR156-Targeted SQUAMOSA PROMOTER BINDING-LIKE  
616 Transcription Factors. *Plant Cell* 24, 3320-3332.

617 Zhang, H.Y., Hu, J.H., Qian, Q., Chen, H., Jin, J., and Ding, Y. (2016a). Small RNA Profiles of  
618 the Rice PTGMS Line Wuxiang S Reveal miRNAs Involved in Fertility Transition.  
619 *Frontiers In Plant Science* 7.

620 Zhang, S.X., Liu, Y.H., and Yu, B. (2015). New insights into pri-miRNA processing and  
621 accumulation in plants. *Wiley Interdisciplinary Reviews-Rna* 6, 533-545.

622 Zhang, W., Xie, Y., Xu, L., Wang, Y., Zhu, X.W., Wang, R.H., Zhang, Y., Muleke, E.M., and Liu,  
623 L.W. (2016b). Identification of microRNAs and Their Target Genes Explores  
624 miRNA-Mediated Regulatory Network of Cytoplasmic Male Sterility Occurrence during  
625 Anther Development in Radish (*Raphanus sativus* L.). *Frontiers In Plant Science* 7.

626 Zhang, Y.-C., Yu, Y., Wang, C.-Y., Li, Z.-Y., Liu, Q., Xu, J., Liao, J.-Y., Wang, X.-J., Qu, L.-H.,  
627 Chen, F., Xin, P., Yan, C., Chu, J., Li, H.-Q., and Chen, Y.-Q. (2013). Overexpression  
628 of microRNA OsmiR397 improves rice yield by increasing grain size and promoting  
629 panicle branching. *Nature Biotechnology* 31, 848-852.

630 Zheng, C.F., Ye, M.X., Sang, M.M., and Wu, R.L. (2019). A Regulatory Network for  
631 miR156-SPL Module in *Arabidopsis thaliana*. *International Journal Of Molecular*  
632 *Sciences* 20.

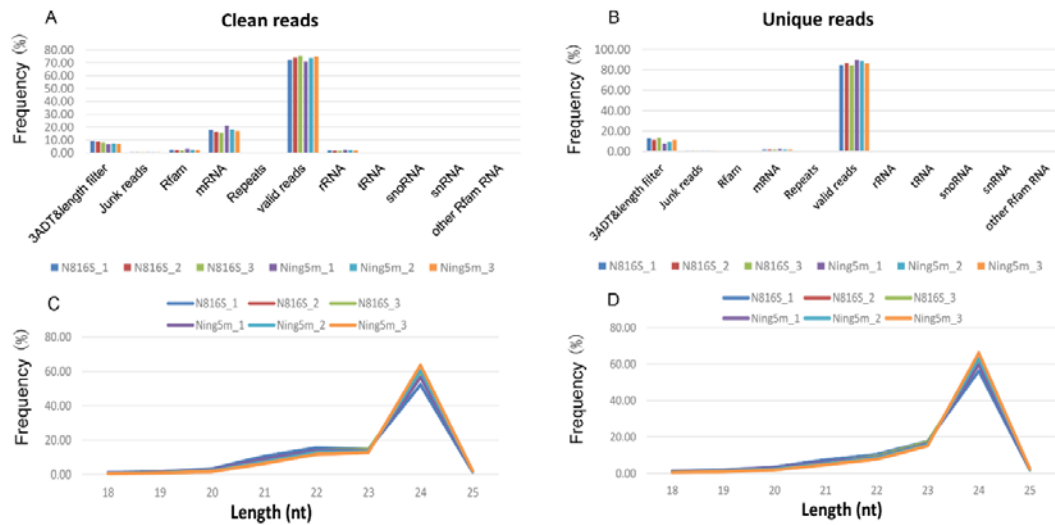
633 Zhou, X.N., Zhang, Z.H., and Liang, X.H. (2020). Regulatory Network Analysis to Reveal  
634 Important miRNAs and Genes in Non-Small Cell Lung Cancer. *Cell Journal* 21,  
635 459-466.

636 Zhu, Q.H., and Helliwell, C.A. (2011). Regulation of flowering time and floral patterning by  
637 miR172. *Journal Of Experimental Botany* 62, 487-495.

638  
639  
640

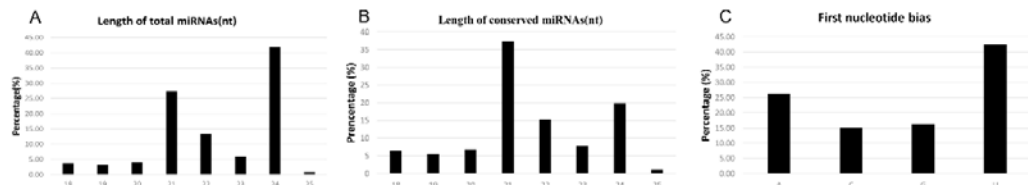
641  
642

## Figures and Tables:



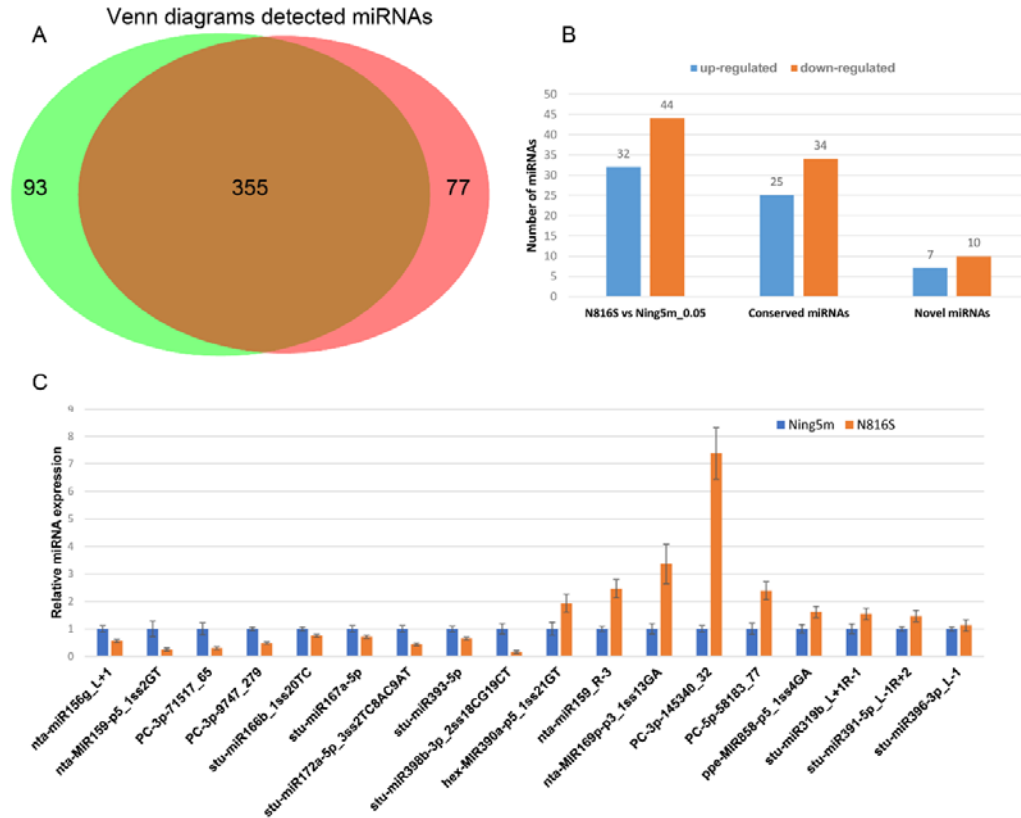
643  
644  
645  
646  
647  
648

Figure 1. Frequency percent of Clean reads (A) and Unique reads (B) sequencing reads, and the length distribution of the clean reads (C) and unique reads (D) from anther of *Capsicum annuum* L.



649  
650  
651  
652  
653  
654

Figure 2. Size distribution of miRNAs and characterization of converted miRNAs detected by deep sequencing. (A) Length distribution of the total miRNAs; (B) Distribution of obtained unique converted miRNAs (gp1-gp3); (C) Percentage of first nucleotide bias in the identified converted miRNAs(gp1-gp3).

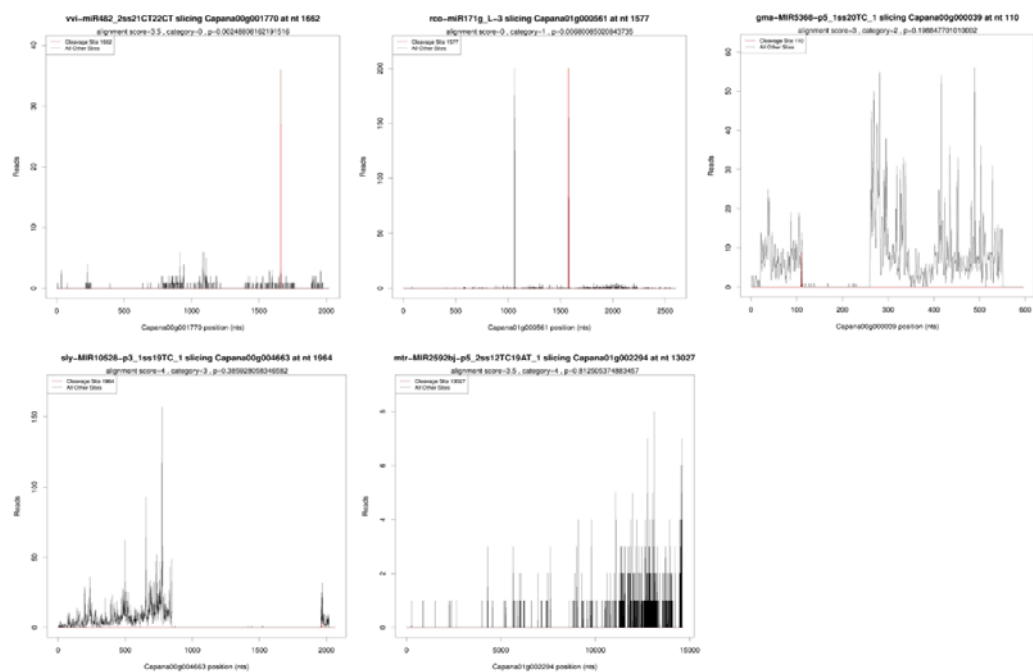


655

656 Figure 3. Venn diagrams detected miRNA, the number statistics of differential  
 657 expression miRNAs, and qRT-PCR for verifying deep sequencing. (A) Detected  
 658 miRNAs in N816S and Ning5m; (B) The number statistics of up-regulated and  
 659 down-regulated differential expression miRNAs in conserved miRNAs and novel  
 660 miRNAs. (C) Detection of selected miRNA expression in N816S and Ning5m anthers  
 661 using qRT-PCR.

662

663



664

665

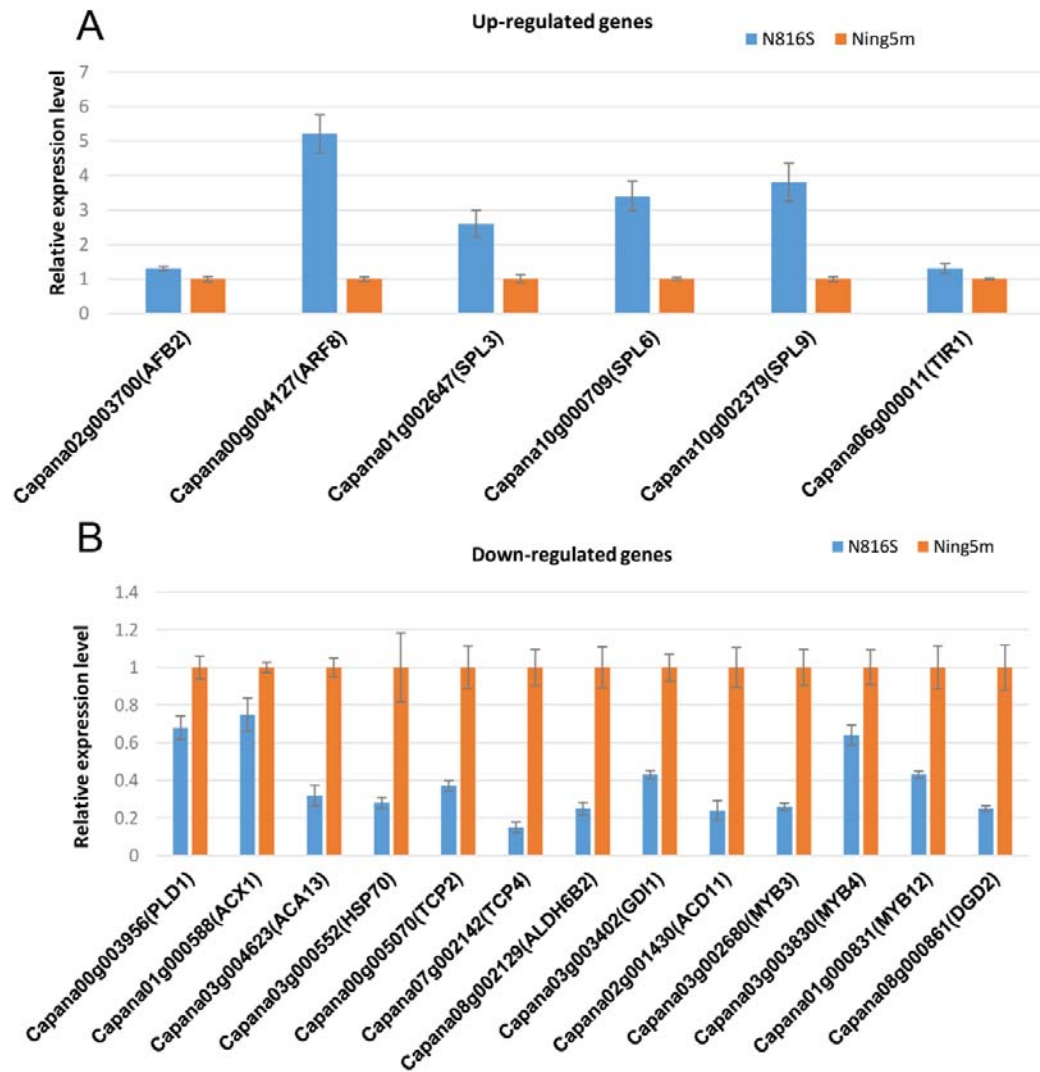
666

667

Figure 4. Typical categories of the target transcript according to the relative abundance of the tags at the target mRNA sites.







676

677 Figure 6. Quantitative real-time PCR analysis of the relative expression of  
678 miRNA targets in the CMS-line N816S and its maintainer line Ning5m. (A)  
679 up-regulated targets in N816S; (B) down-regulated targets in N816S.

680

681

Table 1. Overview of reads from raw data to cleaned sequences.

| Category           | N816S_mean       |                | Ning5m_mean      |                |
|--------------------|------------------|----------------|------------------|----------------|
|                    | Total sRNAs (%)  | unique sRNAs   | Total sRNAs (%)  | unique sRNAs   |
| Raw reads          | 14567767 (100%)  | 8074144 (100%) | 14274100 (100%)  | 7568101 (100%) |
|                    |                  | 1003388        |                  |                |
| 3ADT&Length filter | 1255570 (8.62%)  | (12.43%)       | 1012608 (7.09%)  | 707822 (9.35%) |
| Junk reads         | 74827 (0.51%)    | 54461 (0.67%)  | 74748 (0.52%)    | 54565 (0.72%)  |
| Rfam               | 328527 (2.26%)   | 10516 (0.13%)  | 382951 (2.68%)   | 11080 (0.15%)  |
| mRNA               | 2437774 (16.73%) | 132754 (1.64%) | 2728370 (19.11%) | 138920 (1.84%) |
| Repeats            | 8437 (0.06%)     | 306 (0.00%)    | 8898 (0.06%)     | 293 (0.00%)    |
|                    | 10780898         | 6882786        | 10442445         | 6666094        |
| Valid reads        | (74.01%)         | (85.24%)       | (73.16%)         | (88.08%)       |
| rRNA               | 254459 (1.75%)   | 8362 (0.10%)   | 323537 (2.27%)   | 9018 (0.12%)   |
| tRNA               | 47680 (0.33%)    | 833 (0.01%)    | 32260 (0.23%)    | 786 (0.01%)    |
| snoRNA             | 2925 (0.02%)     | 191 (0.00%)    | 2198 (0.02%)     | 165 (0.00%)    |
| snRNA              | 2671 (0.02%)     | 182 (0.00%)    | 1554 (0.01%)     | 115 (0.00%)    |
| other Rfam RNA     | 20793 (0.14%)    | 948 (0.01%)    | 23402 (0.16%)    | 997 (0.01%)    |

682

683

Table 2. Summary of conserved and predicted miRNA.

| Groups | Pre-miRNA | Unique miRNA | miRNA type      |
|--------|-----------|--------------|-----------------|
| gp1    | 50        | 77           | Conserved miRNA |
| gp2a   | 94        | 122          | Conserved miRNA |
| gp2b   | 314       | 261          | Conserved miRNA |
| gp3    | 35        | 40           | Conserved miRNA |
| gp4    | 421       | 411          | Novel miRNA     |

684

685

Table 3. Summary of the differentially expressed conserved and novel miRNAs.

| MiRNA family | MiRNA name                | N816S(Norm) | Ning5m(Norm) | p_value(t_test) | up/down |
|--------------|---------------------------|-------------|--------------|-----------------|---------|
| miR156       | nta-miR156g_L+1           | 3732.40     | 6752.02      | 0.003           | down    |
|              | han-MIR156b-p3_1ss3CT     | 107.99      | 67.05        | 0.003           | up      |
| MIR159       | stu-miR156a               | 3732.40     | 6752.02      | 0.003           | down    |
|              | nta-MIR159-p5_1ss2GT      | 21.74       | 90.63        | 0.002           | down    |
|              | nta-miR159_R-3            | 384.38      | 160.79       | 0.047           | up      |
| miR162       | csi-miR159a-5p_1ss20AC    | 36.01       | 74.86        | 0.008           | down    |
|              | stu-miR162a-3p            | 5177.75     | 7769.93      | 0.001           | down    |
| miR166       | stu-miR166a-3p_1ss21CA    | 1369.44     | 2506.50      | 0.041           | down    |
|              | stu-miR166b_1ss20TC       | 52460.31    | 71297.86     | 0.029           | down    |
|              | bna-miR166a_L+2           | 49.73       | 83.04        | 0.013           | down    |
|              | aqc-MIR166a-p3_2ss1GC20AC | 26.72       | 19.50        | 0.025           | up      |
|              | aqc-MIR166a-p5_2ss1GC20AC | 26.72       | 19.50        | 0.025           | up      |
|              | nta-miR166a_R+1           | 62.57       | 97.20        | 0.033           | down    |
|              | nta-miR166a_R+1_1ss20CT   | 11.51       | 26.44        | 0.045           | down    |

|          |                                |         |         |       |      |
|----------|--------------------------------|---------|---------|-------|------|
| miR167   | stu-miR167a-5p_1ss21AT         | 44.40   | 62.92   | 0.010 | down |
|          | gma-miR167a_1ss21AT            | 44.40   | 62.92   | 0.010 | down |
|          | aly-miR167a-5p_R+1_1ss21AT     | 0.97    | 6.41    | 0.001 | down |
|          | nta-miR167d_R+2                | 17.46   | 30.80   | 0.040 | down |
|          | mdm-miR167h_1ss22AT            | 0.97    | 6.41    | 0.001 | down |
|          | stu-miR167a-5p                 | 3533.81 | 5033.84 | 0.019 | down |
| MIR169   | nta-MIR169p-p3_1ss13GA         | 15.55   | 4.98    | 0.033 | up   |
| MIR172   | nta-MIR172e-p5_2ss14CG18TA     | 8.43    | 0.64    | 0.002 | up   |
|          | nta-MIR172e-p3_2ss15CG19TA     | 5.31    | 0.00    | 0.048 | up   |
|          | stu-miR172a-5p_3ss2TC8AC9AT    | 21.28   | 49.93   | 0.010 | down |
|          | nta-MIR172f-p5_2ss14CG18TA     | 8.43    | 0.64    | 0.002 | up   |
|          | gra-miR172b_2ss8TC9AT          | 21.28   | 49.93   | 0.010 | down |
| miR319   | stu-miR319-3p_L+2R-2           | 25.71   | 11.69   | 0.018 | up   |
|          | stu-miR319b_L+1R-1             | 4345.23 | 2869.03 | 0.029 | up   |
| MIR390   | hex-MIR390a-p5_1ss21GT         | 186.32  | 99.94   | 0.030 | up   |
|          | hex-MIR390b-p5_2ss10TC21GA     | 10.01   | 4.27    | 0.001 | up   |
|          | hex-MIR390b-p5_1ss21GT         | 186.32  | 99.94   | 0.030 | up   |
| miR391   | stu-miR391-5p_L-1R+2           | 726.92  | 508.13  | 0.009 | up   |
| miR393   | stu-miR393-5p                  | 84.78   | 133.01  | 0.020 | down |
|          | stu-miR393-3p                  | 0.00    | 41.28   | 0.029 | down |
| miR396   | stu-miR396-3p_L-1              | 1503.77 | 1367.94 | 0.038 | up   |
| miR398   | stu-miR398b-3p_2ss18CG19CT     | 1.86    | 12.21   | 0.020 | down |
|          | stu-miR398b-3p                 | 0.00    | 2.70    | 0.021 | down |
| MIR399   | ppe-MIR399a-p5_2ss5AT18TC      | 7.11    | 0.00    | 0.006 | up   |
|          | fve-MIR399b-p5_2ss2GT20GA      | 4.89    | 33.61   | 0.005 | down |
|          | mtr-MIR399b-p5_2ss11TC20TG     | 22.65   | 18.22   | 0.019 | up   |
|          | ppe-MIR399a-p3_2ss5AT18TC      | 7.11    | 0.00    | 0.006 | up   |
|          | stu-miR399j-3p_1ss21GA         | 0.00    | 2.84    | 0.015 | down |
| miR482   | stu-miR482a-5p_1ss12AG         | 158.27  | 274.34  | 0.008 | down |
| MIR858   | ppe-MIR858-p5_1ss4GA           | 611.66  | 386.05  | 0.013 | up   |
| miR1885  | bra-miR1885b                   | 14.61   | 18.27   | 0.007 | down |
| miR3627  | stu-miR3627-5p_R-1             | 8.89    | 0.00    | 0.048 | up   |
| MIR10528 | sly-MIR10528-p3_2ss9GA19TC     | 7.81    | 0.00    | 0.048 | up   |
| MIR11334 | cst-MIR11334-p5_2ss9TG18TC     | 22.54   | 13.15   | 0.025 | up   |
| MIR5141  | rgl-MIR5141-p5                 | 16.53   | 40.47   | 0.023 | down |
| miR6024  | stu-miR6024-3p_R-1_2ss20CT21CT | 20.40   | 9.84    | 0.021 | up   |
| miR6149  | nta-miR6149a_L+1R-1_1ss21GC    | 0.00    | 4.06    | 0.034 | down |
| miR6478  | ptc-miR6478_R-1_1ss20TA        | 4.45    | 0.77    | 0.035 | up   |

|         |                            |        |        |       |      |
|---------|----------------------------|--------|--------|-------|------|
|         | ptc-miR6478_R+3_1ss21GA    | 3.68   | 11.02  | 0.042 | down |
|         | ptc-miR6478_R+2_1ss21GA    | 198.84 | 273.50 | 0.000 | down |
|         | ptc-miR6478_R+1_1ss21GA    | 13.40  | 23.60  | 0.013 | down |
| MIR8005 | stu-MIR8005a-p3_1ss5GA     | 11.39  | 3.39   | 0.036 | up   |
| MIR8021 | stu-MIR8021-p3_2ss15GA22TA | 9.40   | 13.95  | 0.021 | down |
|         | stu-MIR8021-p3_2ss16TC22TG | 26.11  | 35.95  | 0.013 | down |
| miR8175 | ath-miR8175_L+4            | 0.00   | 3.83   | 0.013 | down |
|         | PC-3p-155334_29            | 0.00   | 5.53   | 0.001 | down |
|         | PC-3p-216061_19            | 0.00   | 6.33   | 0.021 | down |
|         | PC-3p-71517_65             | 5.84   | 20.24  | 0.050 | down |
|         | PC-3p-9747_279             | 24.16  | 51.14  | 0.034 | down |
|         | PC-5p-101290_47            | 3.77   | 6.09   | 0.020 | down |
|         | PC-5p-117714_40            | 0.00   | 13.55  | 0.025 | down |
|         | PC-5p-119988_39            | 0.00   | 14.12  | 0.040 | down |
| Novel   | PC-5p-12980_234            | 62.33  | 116.97 | 0.018 | down |
| miRNAs  | PC-5p-347691_9             | 0.00   | 7.12   | 0.040 | down |
|         | PC-5p-567932_5             | 0.00   | 5.04   | 0.014 | down |
|         | PC-3p-145340_32            | 11.33  | 1.54   | 0.014 | up   |
|         | PC-3p-9335_287             | 78.11  | 53.49  | 0.041 | up   |
|         | PC-5p-117747_40            | 11.26  | 1.96   | 0.023 | up   |
|         | PC-5p-153350_30            | 14.73  | 2.06   | 0.010 | up   |
|         | PC-5p-154497_29            | 4.86   | 0.00   | 0.038 | up   |
|         | PC-5p-160111_28            | 9.37   | 1.96   | 0.049 | up   |
|         | PC-5p-58183_77             | 17.38  | 7.49   | 0.030 | up   |

686

687 Note: The miRNA name is composed of the 1st known miRNA name in a cluster, a  
688 underscore, and a matching annotation: such as L-n/+n means the detected miRNA is n base  
689 less or more than known rep\_miRSeq in the left side; R-n/+n means the detected miRNA is n  
690 base less or more than known rep\_miRSeq in the right side; 2ss5TC13TA means 2  
691 substitution (ss), which are T->C at position 5 and T->A at position 13.

692

### 693 **Supporting Information:**

694 Figure S1. Small RNAs Pearson correlation between the six libraries

695 Table S1. Primers used in this study. S1-1, Primers designed for conserved  
696 miRNAs and novel miRNAs; S1-2 Primers designed for miRNA targets.

697 Table S2. Summary of five types of miRNA in this study. S2-1, gp1a type; S2-2,  
698 gp2a type; S2-3, gp2b type; S2-4, gp3 type; S2-5, gp4 type.

699 Table S3. Primers used in this study. S1-1, Primers designed for conserved  
700 miRNAs and novel miRNAs; S1-2, Primers designed for miRNA targets.

701 Table S4. Overview of degradome sequencing reads from raw data to mapping  
702 sequences.

703 Table S5. The overview of reliable identified targets of miRNAs.

704 Table S6. Transcript annotation of targets of differential expression conserved  
705 and novel miRNAs in this study.



706           Table S7. The pathways of all the miRNAs and targets involved in this study.  
707           Table S8. The transcript annotation, GO terms and KEGG pathways of  
708 differential expression miRNAs with those targets in pepper.  
709